PHYSICAL REVIEW B **85**, 081401(R) (2012)

Plasmonic crystals for ultrafast nanophotonics: Optical switching of surface plasmon polaritons

M. Pohl,[1] V. I. Belotelov,[2,3,*] I. A. Akimov,[1,4,†] S. Kasture,[5] A. S. Vengurlekar,[5] A. V. Gopal,[5] A. K. Zvezdin,[3] D. R. Yakovlev,[1,4] and M. Bayer[1]

[1]*Experimentelle Physik 2, Technische Universität Dortmund, D-44221 Dortmund, Germany*
[2]*M.V. Lomonosov Moscow State University, 119991 Moscow, Russia*
[3]*A.M. Prokhorov General Physics Institute, Russian Academy of Sciences, 119992 Moscow, Russia*
[4]*A.F. Ioffe Physical-Technical Institute, Russian Academy of Sciences, 194021 St. Petersburg, Russia*
[5]*Tata Institute of Fundamental Research, 400005, Mumbai, India*

(Received 6 December 2011; published 1 February 2012)

We demonstrate that the dispersion of surface plasmon polaritons in a periodically perforated gold film can be efficiently manipulated by femtosecond laser pulses in spectral regions far from the intrinsic gold resonances. Using a time- and frequency-resolved pump-probe technique we observe shifting of the plasmon polariton resonances with response times from 200 to 800 fs depending on the probe photon energy, by which we obtain comprehensive insight into the electron dynamics in gold. We show that Wood anomalies in the optical spectra provide pronounced resonances in differential transmission and reflection with magnitudes up to 3% for moderate pump fluences of 0.5 mJ/cm^2.

DOI: 10.1103/PhysRevB.85.081401 PACS number(s): 73.20.Mf, 78.47.J−, 78.66.Bz, 78.67.Pt

Nowadays plasmonics attracts much research interest in nanophotonics, inspiring scientists to develop a unique paradigm in data processing based on nanometallic circuitry.[1,2] The key object of plasmonics is the surface plasmon polariton (SPP)—the coupled oscillation of the electromagnetic field and the electron plasma in metals.[3] Excitation of a SPP leads to significant electromagnetic energy localization near the metal-dielectric interface, thereby enhancing nonlinear effects and light-matter interaction. Current state-of-the-art criteria in telecommunications require plasmonics to be active, i.e., a possibility for control by means of an external stimulus must be provided on the order of a few nanoseconds or shorter.[4]

One of the approaches satisfying the strict criteria is magnetoplasmonics employing the influence of an external magnetic field on the SPP propagation constant.[5,6] While the modulation efficiency in magnetoplasmonic structures may be as large as tens of percent, the operation rate is limited by the magnetization dynamics occurring on the nanoseconds time scale. Transient changes in the optical properties of plasmonic structures can be also achieved via application of intense femtosecond laser pulses.[4,7–15] Here, the real and imaginary parts of the dielectric constant of a metal change during several hundreds of femtoseconds.[16–18] Since the propagation constant of SPPs is determined by the permittivity of metal and dielectric, this opens perspectives for ultrafast control of SPPs. However, the high reflectivity of smooth gold surfaces prevents most of the incident electromagnetic energy from being absorbed in the metal. Here, SPPs can be exploited to provide electromagnetic energy localization near the metal-dielectric interface and consequently to increase the energy absorption in gold.[19,20]

Recently the optical response of plasmonic crystals with periodically perforated gold or perforated dielectric on top of gold was investigated by using a two-color pump-probe technique with the pump photon energy detuned from the SPP resonances.[12,13] It was demonstrated that the differential reflectivity of the probe beam tuned in resonance with a SPP can be modulated up to 10% on a subpicosecond time scale. Large values of the modulation parameter were accomplished by using intense laser pulses with a fluence $\Phi \sim 50$ mJ/cm^2 and by tuning the resonances of the probed SPPs close to the d-band transitions in gold [$\hbar\omega_{ib} = 2.3$ eV (Ref. 17)]. However, the drawback of this approach is the large absorption in the vicinity of the d-band transition, resulting in a huge intrinsic SPP damping. A similar obstacle, but with even larger optical losses, occurs in Al plasmonic crystals.[21]

Here, we demonstrate that the dielectric constant of the metal in a plasmonic crystal can be efficiently modified at the femtosecond time scale via SPP excitation, leading to ultrafast modification of the SPP dispersion. This is possible in spectral ranges far from the intrinsic resonance frequencies of the metal system. From the temporal and spectral dependence of differential reflectivity and transmission we extract comprehensive information on the electron energy relaxation in gold. We achieve a 3% probe intensity modulation with about an order of magnitude smaller pump fluence of $\Phi \approx 0.5$ mJ/cm^2 as compared to previous works.[13]

The investigated plasmonic crystal is schematically shown in Fig. 1(a). It comprises a periodically perforated, 120-nm-thick gold film deposited on top of a smooth ferromagnetic layer of rare-earth iron-garnet BiIG with 2.5-μm thickness. The period is $d = 595$ nm with a groove depth of 120 nm and an air groove width of 110 nm.[22] The time-resolved differential transmission and reflection were measured by a pump-probe technique using a Ti-Sa laser with a pulse repetition rate of about 80 MHz, a center wavelength around 800 nm, and a pulse duration of $\tau_D = 30$ fs.[22] In the experiment the pump beam entered the sample in the plane perpendicular to the slits, while the probe beam was incident in the slit plane [Fig. 1(a)]. The incidence angles θ_1 and θ_2 for both the pump and probe were set to 17°, with an aperture angle around 6°. The plasmonic crystal was designed to have SPP resonances in the energy range 1.5–1.7 eV for both the pump and probe beams in this configuration.

Zero-order transmission and reflection spectra measured using a spectrally broad halogen lamp are shown in

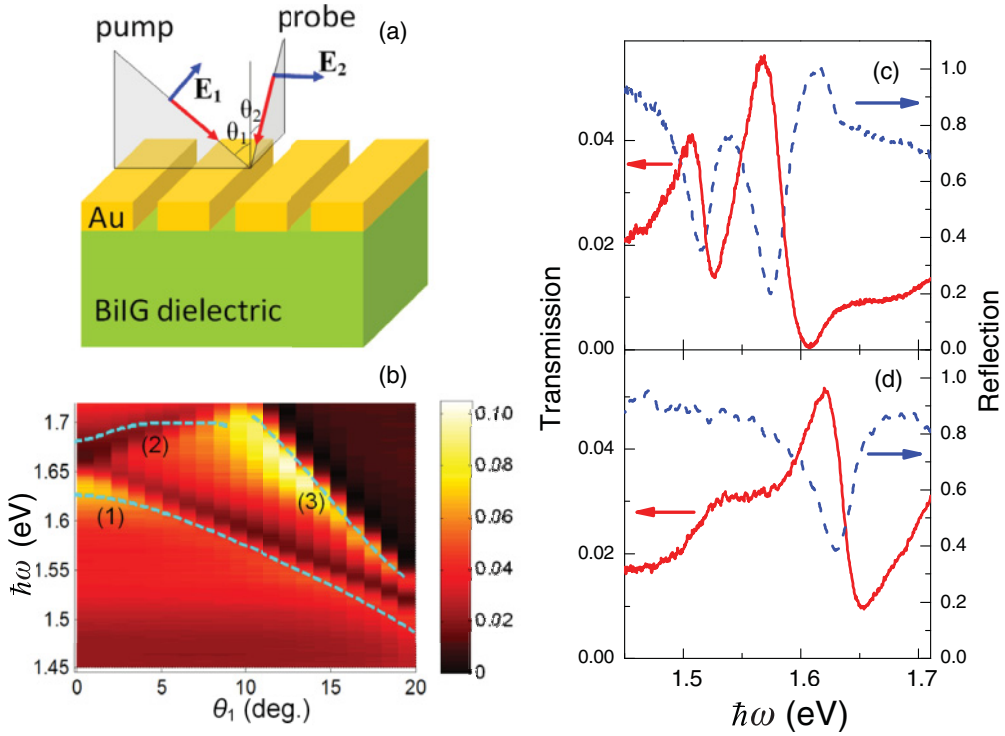

FIG. 1. (Color online) (a) Scheme of the plasmonic crystal for active control of SPPs. (b) Contour plot of zero-order transmission vs photon energy and angle of incidence θ_1 measured in the pump configuration. Dispersion of the SPP propagating at the BiIG/Au [(1), (2) dashed curves] and at the Au/air [(3) dashed curve] interfaces calculated by the S-matrix method. (c), (d) Experimentally measured transmission (solid lines) and reflection (dashed lines) spectra for the pump (c) and probe (d) configurations at an incidence angle of 17°. The incident light is p polarized in (c) and s polarized in (d).

Figs. 1(b)–1(d). They demonstrate resonances with an asymmetric Fano-like shape.[23] The dispersion of these resonances is seen from Fig. 1(b), presenting transmission spectra measured at different incidence angles for illumination in the pump configuration. The angular dependence of the energy position of these resonances corresponds well to the dispersion of the SPP modes calculated with the scattering matrix (S-matrix) method[24,25] [dashed curves in Fig. 1(b)]. Consequently, these features can be referred to as Wood anomalies[26] related to the SPPs. The pump beam excites the SPPs in the fourth band of the Au/dielectric interface [curve (1) in Fig. 1(b)] and the second band SPP at the Au/air interface [curve (3) in Fig. 1(b)] with an energy around 1.55 eV. On the other hand, the transmission spectrum of the probe beam does not show any pronounced dependence on the incidence angle. It is approximately the same at $\theta_2 = 17°$ as the transmission spectrum of the pump beam at $\theta_1 = 0°$ [compare Fig. 1(d) with the corresponding cut of Fig. 1(b) at $\theta_1 = 0°$]. Since the probe beam is incident along the slits, it transfers zero momentum to the SPP which corresponds to $\theta_1 = 0°$ in the dispersion diagram, and indicates that the probe beam interacts with the SPPs in the fourth band of the Au/dielectric interface at 1.63 eV. It should be noted that in plasmonic crystals both localized and propagating SPPs can be excited.[6,27] In our case we deal with propagating SPPs, which follows from the plasmonic resonance dispersion shown in Fig. 1(b).

Plasmonic crystals possess extraordinary optical transmission and, therefore, transient changes in the gold permittivity can be monitored not only in reflection but also in transmission. Since SPPs are TM polarized they can be excited only by p polarization of the pump beam or by s polarization of the probe beam. This is also illustrated by the electromagnetic field distribution in the crystal.[22] The strongest transient signals of differential transmission $\Delta T/T$ and reflection $\Delta R/R$ are expected in the case when both the pump and probe excite SPPs. Indeed, a pump SPP allows significant electromagnetic energy absorption in gold, whereas a probe SPP causes Fano resonances in T and R spectra. The latter increases the sensitivity of the transient signals due to the changes in the optical properties of gold. Experimental results prove this statement unambiguously (Fig. 2). As expected, the signal is strongest for the fully plasmonic configuration (p,s) (p and s polarizations of the pump and probe, respectively). Compared to this configuration the signal strongly decreases for all other polarization combinations of the pump and probe.[28]

The signal in the totally nonplasmonic case of the s-polarized pump and p-polarized probe can be hardly seen. In the (p,p) case the SPP is excited by the pump beam, but the changes in reflectivity and transmission are more than one order of magnitude smaller. This is explained by the weak sensitivity of both transmitted and reflected probe beams due to the absence of resonances in the probed spectrum, and demonstrates the importance of SPPs for transient optical property sensing. Finally, in the (s,s) configuration a plasmonic resonance is present in the T and R spectra, but the signal

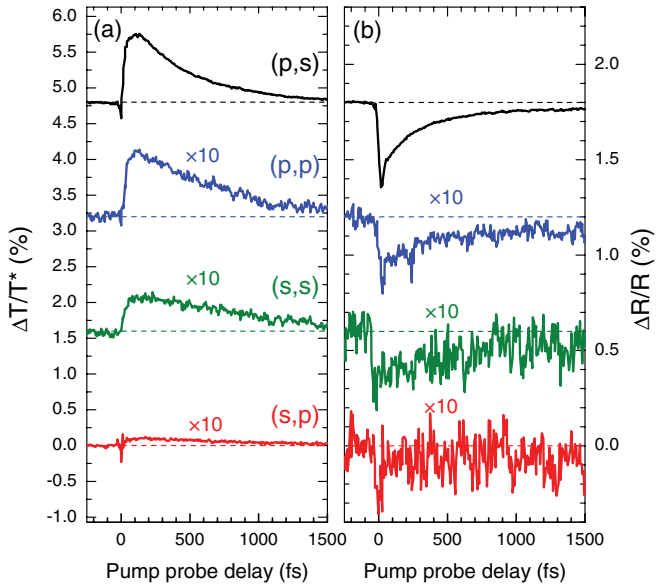

FIG. 2. (Color online) Time-resolved differential transmission (a) and reflectivity (b) signals measured for different polarization configurations of pump and probe beams. The signals are shifted vertically for clarity (zero levels are shown by dashed lines). The signals for (p,p), (s,s), and (s,p) configurations are multiplied by 10. The pump fluence here and for the experimental results in all subsequent figures is 0.5 mJ/cm^2.

is still as small as in the (p,p) configuration. This manifests the importance of SPP excitation by the pump beam, which provides an efficient trapping of the incident photons and their consecutive absorption in the gold.

The transients $\Delta T/T$ and $\Delta R/R$ versus time t can be well described by a sum of two contributions

$$\frac{\Delta I}{I}(t) = D_j e^{-[\frac{t}{\sigma}]^2} + \frac{A_j}{2}\left[1+\mathrm{erf}\left(\frac{t}{\sigma}-\frac{\sigma}{2\tau_j}\right)\right] e^{[\frac{\sigma}{2\tau_j}]^2-\frac{t}{\tau_j}} + \frac{B_j}{2}\left[1+\mathrm{erf}\left(\frac{t}{\sigma}\right)\right], \quad (1)$$

where $I = R,T$, $j = R,T$, erf is the Gaussian error function, and τ_j is the relaxation time. We assume that the pulse intensity has a Gaussian profile with a full width half maximum $\tau_D = \sqrt{2\ln 2}\sigma$. Here, the first term corresponds to a fast instantaneous component, which follows the autocorrelation function of the laser pulses. This component is also present in the $\Delta R/R$ from flat gold when the pump and probe are incident from the magnetic film side. Therefore, we attribute this signal to the nonlinear optical response from the magnetic film related with optical transitions in octahedrally coordinated Fe^{3+} ions.[29] The next contribution is described by the second and the third terms in Eq. (1), and manifests a fast increase of the signal followed by a monotonous decay to a plateau. This contribution is associated with optically induced excitation of electrons and their energy relaxation in gold. It can be described by a multiexponential decay convoluted with the apparatus function.[30] For simplicity, we consider this optical response as a single exponential decay with amplitude A_j and decay time τ_j reaching a plateau at the level B_j.

The polarization properties (see Fig. 2) directly show the major role of SPPs for efficient energy absorption and high probe sensitivity. Consequently, the spectral dependence of the transient signals should also reflect resonant behavior and have extrema in the vicinity of the plasmonic resonances. In order to check this, we introduced an electrically tunable interference filter (20-meV bandwidth) in the reflected and transmitted probe beam, directly in front of the photodetector. Thereby, we were able to probe the evolution of the SPP resonances after absorption of the pump pulse [see Figs. 3(a) and 3(b)]. Both $\Delta T/T$ and $\Delta R/R$ signals change sign at around 1.60–1.66 eV. This is clearly seen from the spectral dependencies of the coefficients A_T and A_R, which are shown in Fig. 3(c). Such behavior can be explained by a shift of the Fano resonance along with a broadening. Surprisingly, the relaxation times τ_T and τ_R also vary with energy [Fig. 3(d)]. This indicates that the relative contributions of different parts of the transient permittivity ϵ_m of metal to $\Delta T/T$ and $\Delta R/R$ are energy dependent.

In order to explain the spectral and temporal dependencies of the differential signals we consider the response of the dielectric function in gold under ultrafast optical excitation by pump pulses. Here it is necessary to take into account two types of excitation processes: (i) intraband electron transitions within the conduction band and (ii) interband transitions of electrons between the d and conduction bands.[17] Accordingly the dielectric constant of gold in the Drude model, including interband transitions, is given by

$$\epsilon_m = 1 - \frac{\omega_p^2}{\omega(\omega+i\gamma)} + \chi_1^{ib} + i\chi_2^{ib}, \quad (2)$$

where ω_p is the plasma frequency, γ is the electron scattering rate, and χ_1^{ib} and $i\chi_2^{ib}$ are the real and imaginary parts of the interband susceptibility. While χ_2^{ib} is centered around the electron d-band transition frequency, χ_1^{ib} is spread in frequency and gives noticeable contributions to ϵ_m even far from the d-band transition in gold.[31]

Intraband absorption gives rise to a strong nonequilibrium electron distribution around the Fermi energy.[17] Due to electron-electron scattering, electron thermalization takes place, leading to a hot Fermi distribution. Simultaneous to the internal electron thermalization, electron-phonon interactions transfer energy to the lattice during ~1 ps. This process leads to the transient changes in χ_1^{ib}. The value of $\Delta\chi_1^{ib}$ is approximately proportional to the integrated absorption of the laser pulse and evolves in parallel with the electron-lattice thermalization.[19] Intraband absorption also changes the scattering rate γ. However, the temporal behavior of $\Delta\gamma$ is different from the one for $\Delta\chi_1^{ib}$. While $\Delta\chi_1^{ib}$ reaches its maximum as soon as the pump pulse is finished, $\Delta\gamma$ increases during the first hundred femtoseconds and then decreases on time scales much larger than 1 ps.[18] This is due to the fact that at earlier stages $\Delta\gamma$ is mainly due to the heating of the electron and phonon systems, while for the subsequent stages it is dominated by energy relaxation of these systems via electron-phonon and phonon-phonon interactions.[16] Along with the excitation of conduction electrons, there is also interband absorption as long as $\hbar\omega_1 + \hbar\omega_2 > \hbar\omega_{ib}$, which is

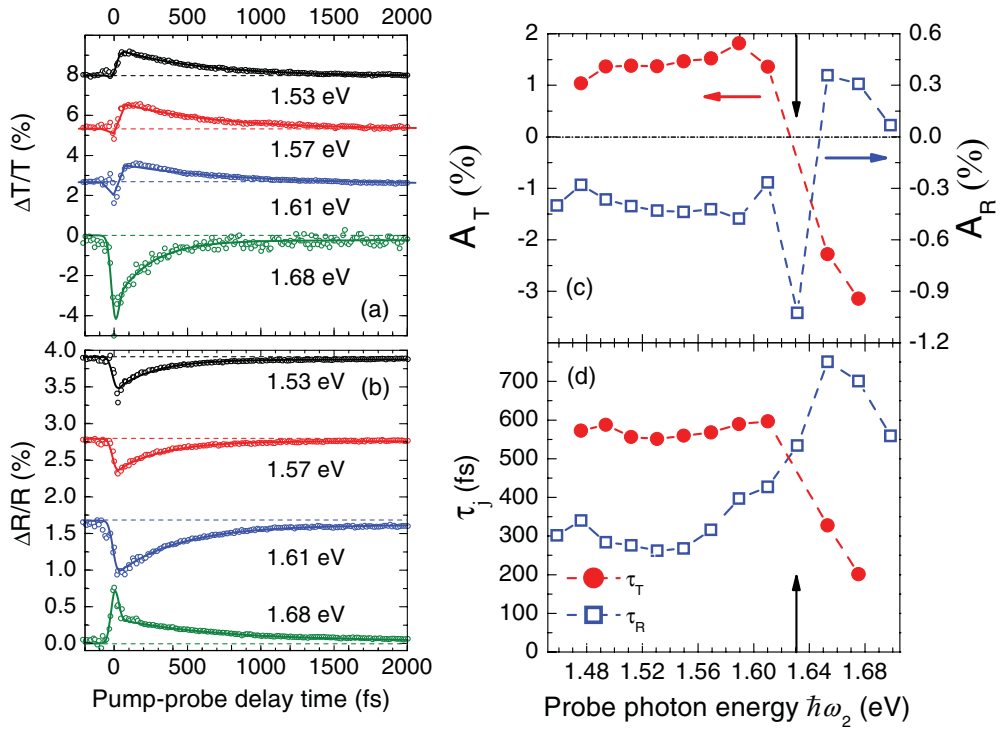

FIG. 3. (Color online) Left: Transient transmission (a) and reflection (b) at different probe energies $\hbar\omega_2 = 1.53$, 1.57, 1.61, and 1.68 eV. The solid lines are fits with Eq. (1). Right: Spectral dependencies of the amplitudes A_j (c) and the decay times τ_j (d) of the transient signal in transmission ($j = T$, solid symbols) and reflection ($j = R$, open symbols) evaluated from fits of the experimental data. Vertical arrows indicate the energy of the probe SPP.

satisfied for our case. This leads to ultrafast changes in χ_2^{ib} lasting shorter than a hundred femtoseconds.[18]

It follows from the experimental data in Figs. 2 and 3 that we probe the optical response of SPP resonances, occurring due to pump-induced changes of ϵ_m as described above. Since $\Delta\gamma$ relaxes during times much longer than several picoseconds (which is out of the observation range), this causes a plateau in the transient signals described by B_j in Eq. (1). On the contrary, $\Delta\chi_1^{ib}$ relaxes much faster ($\sim$1 ps) and contributes to the exponential decay with the amplitudes A_j in Eq. (1). Similarly, $\Delta\chi_2^{ib}$ also contributes to A_j on a time scale of 100 fs. Thus, in the perturbation regime the A_j can be written as a linear combination of $\Delta\chi_1^{ib}$ and $\Delta\chi_2^{ib}$ with frequency-dependent coefficients $C_{1,j}(\omega)$ and $C_{2,j}(\omega)$:

$$A_j(\omega) = C_{1,j}(\omega)\frac{\Delta\chi_1^{ib}}{\chi_1^{ib}} + C_{2,j}(\omega)\frac{\Delta\chi_2^{ib}}{\chi_2^{ib}}. \qquad (3)$$

In our experiments the pump energy is far from the d-band transitions in gold so that χ_1^{ib} and χ_2^{ib} can be considered constant for the energy range of interest. The spectral behavior of the coefficients in Eq. (3) can be determined by modeling T and R spectra applying a rigorous coupled-wave analysis (RCWA).[32] Equation (3) gives the best fits of $A_j(\omega)$ for $\Delta\chi_1^{ib}/\chi_1^{ib} = 0.4 \times 10^{-2}$, and $\Delta\chi_2^{ib}/\chi_2^{ib} = 2.6 \times 10^{-2}$ (Fig. 4).

It is seen from Fig. 4 that the relative contributions of $\Delta\chi_1^{ib}$ and $\Delta\chi_2^{ib}$ determined by $C_{1,j}(\omega)\Delta\chi_1^{ib}/\chi_1^{ib}$ and $C_{2,j}(\omega)\Delta\chi_2^{ib}/\chi_2^{ib}$ are energy dependent. In the energy range of 1.45–1.60 eV, the term $C_{1,T}(\omega)\Delta\chi_1^{ib}/\chi_1^{ib}$ prevails in absolute value over the term $C_{2,T}(\omega)\Delta\chi_2^{ib}/\chi_2^{ib}$ and the term $C_{2,R}(\omega)\Delta\chi_2^{ib}/\chi_2^{ib}$ prevails over the term $C_{1,R}(\omega)\Delta\chi_1^{ib}/\chi_1^{ib}$. At higher energies of 1.60–1.66 eV these ratios get reversed. Since different contributions have different relaxation times, this leads to the energy dependence of τ_j. As discussed above, $\Delta\chi_2^{ib}$ relaxes in less than a hundred of femtoseconds, which diminishes τ_j. This explains the experimentally observed drop of τ_T for larger energies where $\Delta\chi_2^{ib}$ contributes more strongly to Eq. (3) [see Fig. 3(d)]. The decrease of τ_R for smaller energies can be explained similarly by the stronger contribution of $\Delta\chi_2^{ib}$.

Furthermore, the significantly different temporal behaviors of $\Delta\gamma$ and $\Delta\chi_2^{ib}$ allow us even to discriminate their input in the differential signals. The coefficients B_j in Eq. (1) give a $\Delta\gamma/\gamma = 3.0 \times 10^{-2}$ corresponding to $\Delta\gamma/\Delta\chi_2^{ib} = 1.15$. This is in agreement with the data in Ref. 18, providing $\Delta\gamma/\Delta\chi_2^{ib} \approx 1$.

In conclusion, we show that the optical properties of plasmonic crystals can be tuned by femtosecond laser pulses. As a result, SPP propagation through the plasmonic crystal is modified and corresponding differential transmission and reflection changes of the order of 3% are observed. The response time of plasmonic crystals can be varied widely from 200 to 800 fs by tuning the relative spectral positions of the probe and the SPP resonance. An analysis of transient optical spectra along with a rigorous solution of Maxwell's equations provides sufficient information for determining the magnitude and the ultrafast optical response of the gold permittivity.

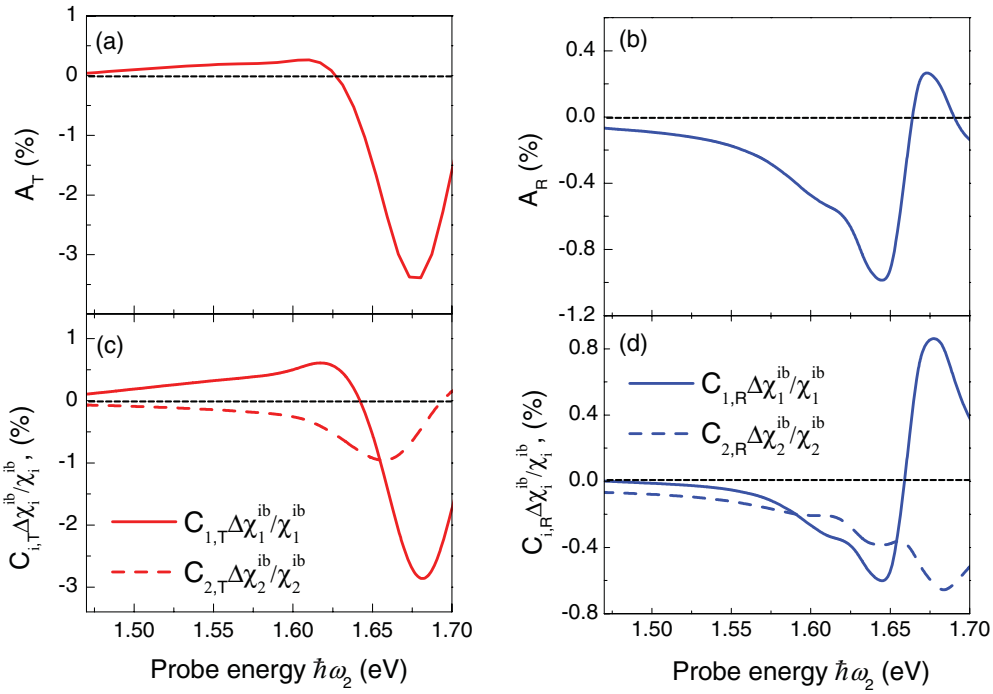

FIG. 4. (Color online) Spectral dependencies of A_T (a) and A_R (b) obtained by RCWA modeling, to have the best correspondence with the experimental data. (c), (d) Spectral dependencies of different contributions related with $\Delta\chi_1^{ib}$ ($i = 1$, solid lines) and $\Delta\chi_2^{ib}$ ($i = 2$, dashed lines) in accordance with Eq. (3).

The authors are grateful to M. Betz for discussions. The work is supported by the Deutsche Forschungsgemeinschaft, Russian Foundation of Basic Research, DST (India), the Russian Presidential Grant No. MK-3123.2011.2, and by the Federal Targeted Program (No. 16.740.11.0577).

*belotelov@physics.msu.ru
†ilja.akimov@tu-dortmund.de

[1] M. L. Brongersma and V. M. Shalaev, Science **328**, 440 (2010).
[2] J. A. Schuller, E. S. Barnard, W. Cai, Y. C. Jun, J. S. White, and M. L. Brongersma, Nat. Mater. **9**, 193 (2010).
[3] S. A. Maier, *Plasmonics—Fundamentals and Applications* (Springer, New York, 2007).
[4] K. F. MacDonald, Z. L. Sámson, M. I. Stockman, and N. I. Zheludev, Nat. Photonics **3**, 55 (2009).
[5] V. V. Temnov, G. Armelles, U. Woggon, D. Guzatov, A. Cebollada, A. Garcia-Martin, J.-M. Garcia-Martin, T. Thomay, A. Leitenstorfer, and R. Bratschitsch, Nat. Photonics **4**, 107 (2010).
[6] V. Belotelov, I. Akimov, M. Pohl, V. Kotov, S. Kasture, A. Vengurlekar, A. Gopal, D. Yakovlev, A. Zvezdin, and M. Bayer, Nat. Nanotechnol. **6**, 370 (2011).
[7] C. Ropers, D. J. Park, G. Stibenz, G. Steinmeyer, J. Kim, D. Kim, and C. Lienau, Phys. Rev. Lett. **94**, 113901 (2005).
[8] M. van Exter and A. Lagendijk, Phys. Rev. Lett. **60**, 49 (1988).
[9] Z. L. Sámson, K. F. MacDonald, and N. I. Zheludev, J. Opt. A **11**, 114031 (2009).
[10] O. Muskens, N. Del Fatti, and F. Vallée, Nano Lett. **6**, 552 (2006).
[11] J. N. Caspers, N. Rotenberg, and H. M. van Driel, Opt. Express **18**, 19761 (2010).
[12] N. Rotenberg, M. Betz, and H. M. van Driel, Opt. Lett. **33**, 2137 (2008).
[13] N. Rotenberg, J. N. Caspers, and H. M. van Driel, Phys. Rev. B **80**, 245420 (2009).
[14] H. Baida, P. Billaud, S. Marhaba, D. Christofilos, E. Cottancin, A. Crut, J. Lerme, P. Maioli, M. Pellarin, M. Broyer, N. D. Fatti, and F. Vallée, Nano Lett. **9**, 3463 (2009).
[15] A. Deviis and V. Gulbinas, Appl. Opt. **47**, 1632 (2008).
[16] N. Del Fatti, R. Bouffanais, F. Vallée, and C. Flytzanis, Phys. Rev. Lett. **81**, 922 (1998).
[17] C. K. Sun, F. Vallée, L. H. Acioli, E. P. Ippen, and J. G. Fujimoto, Phys. Rev. B **50**, 15337 (1994).
[18] N. Del Fatti, C. Voisin, M. Achermann, S. Tzortzakis, D. Christofilos, and F. Vallée, Phys. Rev. B **61**, 16956 (2000).
[19] R. H. M. Groeneveld, R. Sprik, and A. Lagendijk, Phys. Rev. B **51**, 11433 (1995).
[20] X. Liu, R. Stock, and W. Rudolph, Phys. Rev. B **72**, 195431 (2005).
[21] A. S. Kirakosyan, M. Tong, T. V. Shahbazyan, and Z. V. Vardeny, Appl. Phys. B **93**, 131 (2008).
[22] See Supplemental Material at http://link.aps.org/supplemental/10.1103/PhysRevB.85.081401 for experimental details and electromagnetic field distributions.
[23] B. Luk'yanchuk, N. Zheludev, S. Maier, N. Halas, P. Nordlander, H. Giessen, and C. Chong, Nat. Mater. **9**, 707 (2010).

[24] S. G. Tikhodeev, A. L. Yablonskii, E. A. Muljarov, N. A. Gippius, and T. Ishihara, Phys. Rev. B **66**, 045102 (2002).

[25] V. Belotelov, D. Bykov, L. Doskolovich, A. Kalish, and A. Zvezdin, JETP **110**, 816 (2010).

[26] R. W. Wood, Phys. Rev. **48**, 928 (1935).

[27] S. Linden, J. Kuhl, and H. Giessen, Phys. Rev. Lett. **86**, 4688 (2001).

[28] Here, the T of the probe for the nonplasmonic case is much smaller, and therefore for adequate comparison of all configurations, the transient signal in transmission was normalized by the transmission for the case of s-polarized probe T^*.

[29] A. M. Grishin and S. I. Khartsev, Appl. Phys. Lett. **95**, 102503 (2009).

[30] R.Wilks and R. Hicken, J. Phys. Condens. Matter **16**, 4607 (2004).

[31] A. Pinchuk, G. Plessen, and U. Kreibig, J. Phys. D **37**, 3133 (2004).

[32] M. G. Moharam, D. A. Pommet, E. B. Grann, and T. K. Gaylord, J. Opt. Soc. Am. A **12**, 1077 (1995).